Hyperbolic Delaunay complexes and Voronoi diagrams made practical

Mikhail Bogdanov, Olivier Devillers, Monique Teillaud

▶ **To cite this version:**

Mikhail Bogdanov, Olivier Devillers, Monique Teillaud. Hyperbolic Delaunay complexes and Voronoi diagrams made practical. [Research Report] RR-8146, 2012. hal-00756522v1

HAL Id: hal-00756522

https://inria.hal.science/hal-00756522v1

Submitted on 23 Nov 2012 (v1), last revised 5 Dec 2012 (v2)

HAL is a multi-disciplinary open access archive for the deposit and dissemination of scientific research documents, whether they are published or not. The documents may come from teaching and research institutions in France or abroad, or from public or private research centers.

L'archive ouverte pluridisciplinaire **HAL**, est destinée au dépôt et à la diffusion de documents scientifiques de niveau recherche, publiés ou non, émanant des établissements d'enseignement et de recherche français ou étrangers, des laboratoires publics ou privés.

Hyperbolic Delaunay complexes and Voronoi diagrams made practical

Mikhail Bogdanov, Olivier Devillers, Monique Teillaud

RESEARCH REPORT
N° 8146
December 2012
Project-Team Geometrica

ISSN 0249-6399 ISRN INRIA/RR--8146--FR+ENG

Hyperbolic Delaunay complexes and Voronoi diagrams made practical

Mikhail Bogdanov, Olivier Devillers, Monique Teillaud

Project-Team Geometrica

Research Report n° 8146 — December 2012 — 27 pages

Abstract: We study Delaunay complexes and Voronoi diagrams in the Poincaré ball, a confomal model of the hyperbolic space, in any dimension. We elaborate on our earlier work on the space of spheres [15], giving a detailed description of algorithms, and presenting a static and a dynamic variants. All proofs are based on geometric reasoning, they do not resort to any use of the analytic formula of the hyperbolic distance. We also study algebraic and arithmetic issues, observing that only rational computations are needed. This allows for an exact and efficient implementation in 2D. All degenerate cases are handled. The implementation will be submitted to the CGAL editorial board for future integration into the CGAL library.

Key-words: Hyperbolic geometry, Poincaré ball, Space of spheres.

RESEARCH CENTRE
SOPHIA ANTIPOLIS – MÉDITERRANÉE

2004 route des Lucioles - BP 93
06902 Sophia Antipolis Cedex

Complexes de Delaunay et diagramme de Voronoï hyperboliques en pratique

Résumé : Nous étudions les complexes de Delaunay et les diagrammes de Voronoï dans la boule de Poincaré, modèle conforme de l'espace hyperbolique, en dimension quelconque. Nous étendons notre travail précédent sur l'espace des sphères [15] en donnant une description détaillée des algorithmes, et en présentant des variantes statiques et dynamiques. Toutes les démonstrations reposent sur des raisonnements géométriques et n'utilisent pas de formules analytiques d'expression de la distance hyperbolique. Nous étudions également les aspects algébriques et arithmétiques et observons que tous les calculs nécéssaires peuvent être effectués avec des nombres rationnels. Cela nous permet d'obtenir une implémentation exacte et efficace gérant tous les cas dégénérés. L'implémentation sera soumise au comité éditorial de CGAL pour une intégration future dans la bibliothèque CGAL.

Mots-clés : Géométrie hyperbolique, boule de Poincaré, espace des sphères.

1 Introduction

As D. Eppstein states: "Hyperbolic viewpoint may help even for Euclidean problems" [20].[1] He gives two examples: the computation of 3D Delaunay complexes of sets lying in two planes [8], and optimal Möbius transformation and conformal mesh generation [6]. Hyperbolic geometry is also used in applications like graph drawing [27, 21].

Several years ago, we showed that the hyperbolic Delaunay complex and Voronoi diagram can easily be deduced from their Euclidean counterparts [15, 8]. As far as we know, this was the first time when the computation of hyperbolic Delaunay complexes and Voronoi diagrams was addressed. Since then, the topic appeared again in many publications. Onishi and Takayama write that they "rediscover the algorithm of [15]", in a way that they consider as "more natural", ie. their proofs rely only on algebraic computations instead of geometric reasoning [29]. Nielsen and Nock transform the computation of the Voronoi diagram in the non-conformal Klein model to the computation of an Euclidean power diagram [28]; however, even when the input sites have rational coordinates, the weighted points on which the power diagram is computed have algebraic coordinates. Many other references can be found in [32] (which does not mention [15, 8], though).

None of the above papers shows interest in practical aspects, especially algebraic and arithmetic aspects, which are well known to be crucial for exactness and efficiency of implementations.

In this paper, we stick to the Poincaré ball model of the hyperbolic space, which is *conformal*, ie., preserves hyperbolic angles. Due to this property, the model is used in a wide range of applications (see for instance [26, 39, 25]). We elaborate on our preliminary work [7, 15, 8], giving a detailed description of algorithms allowing to compute the hyperbolic Delaunay complex and Voronoi diagram in any dimension, either in a static or in a dynamic setting. All degenerate cases are handled. All proofs rely on purely geometric proofs, avoiding any computation and any use of the hyperbolic distance formulas. We show that only simple arithmetic computations on rational numbers are needed. The algorithm was implemented in 2D in an exact and efficient way. The implementation will soon be submitted to the CGAL editorial board for future integration into the CGAL library.

We first recall some background on the space of spheres (Section 2), Euclidean Voronoi diagrams and Delaunay triangulations. Section 3 recalls basics on hyperbolic geometry, and their interpretation in the space of spheres. In Section 4, we study hyperbolic Voronoi diagrams and Delaunay complexes, and we present algorithms. Section 5 shows, using geometric reasoning, that the computation and embedding of hyperbolic Delaunay complexes and Voronoi diagrams only use rational computations, but for Voronoi vertices whose coordinates are algebraic numbers of degree two. Section 6 presents the implementation, it gives precisions on algebraic and arithmetic aspects, and presents experimental results, in dimension 2.

2 The space of spheres

$\mathbb{E}^d$ denotes the d-dimensional Euclidean space, $< ., . >$ the scalar product, and $\|.\|$ the Euclidean norm.

The space of spheres states a correspondence between spheres of $\mathbb{E}^d$ and points of $\mathbb{E}^{d+1}$ [5, Chapter 20] [15]. Let χ denote the last coordinate in the space of spheres $\mathbb{E}^{d+1}$. The direction of the χ-axis is called *vertical*.

An Euclidean sphere S centered at c with radius r is denoted as $S = (c, r)$ and has equation $S(x) = 0$ in $\mathbb{E}^d$, where:

$$S(x) = \|x\|^2 - 2 < c, x > + \|c\|^2 - r^2.$$

[1] see also `http://www.ics.uci.edu/~eppstein/pubs/geom-hyperbolic.html`

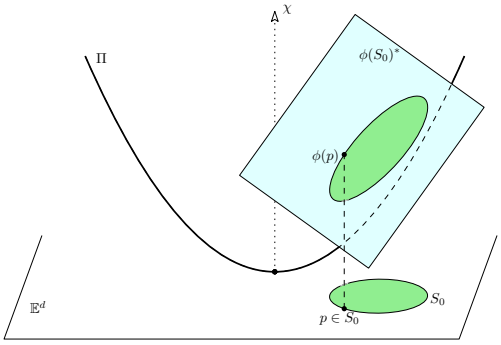

Figure 1: The space of spheres.

The map ϕ associates S to the point

$$\phi(S) = (c, \chi) \in \mathbb{E}^{d+1}, \quad \chi = \|c\|^2 - r^2.$$

We can embed $\mathbb{E}^d$ into $\mathbb{E}^{d+1}$ by identifying it with the hyperplane $\chi = 0$. By the embedding, $\phi(S) \in \mathbb{E}^{d+1}$ projects vertically on $\mathbb{E}^d$ to the center c of S. The points of $\mathbb{E}^d$, considered as spheres of null radius, map by ϕ to the unit paraboloid of $\mathbb{E}^{d+1}$

$$\Pi : \chi = \|c\|^2 .$$

Spheres of $\mathbb{E}^d$ map to points below Π, whereas a point above Π corresponds to an imaginary sphere, ie., a sphere whose radius is an imaginary complex number.

The *pencil of spheres* determined by two spheres S_1 and S_2 is the set of spheres whose equations are the affine combinations of the equations of S_1 and S_2:

$$S: \quad S(x) = \alpha \cdot S_1(x) + (1 - \alpha) \cdot S_2(x), \quad \alpha \in \mathbb{E}.$$

This pencil is mapped by ϕ to the line through $\phi(S_1)$ and $\phi(S_2)$ in the space of spheres.

The set of spheres of $\mathbb{E}^d$ orthogonal to a given sphere S_0 is represented in $\mathbb{E}^{d+1}$ by the polar hyperplane $\phi(S_0)^*$ of point $\phi(S_0) = (c_0, \chi_0)$ with respect to Π. The equation of this polar hyperplane is obtained by polarizing the equation of Π in S_0 (see Figure 1):

$$\phi(S_0)^* : \frac{\chi + \chi_0}{2} = < c_0, c > .$$

In particular, a point (seen as a sphere of null radius) and a sphere are orthogonal if and only if the point lies on the sphere. The intersection of $\phi(S_0)^*$ and Π is the image by ϕ of the set of points of $\mathbb{E}^d$ lying on S_0, ie., $\phi(S_0)^* \cap \Pi$ vertically projects on $\mathbb{E}^d$ to S_0. For a point $p \in \mathbb{E}^d$, the set of spheres passing through p maps to the hyperplane $\phi(p)^*$ tangent to Π at point $\phi(p) \in \Pi$.

The lower half space of $\mathbb{E}^{d+1}$ limited by $\phi(p)^*$ (i.e. the half space which does not contain Π) represents the spheres of $\mathbb{E}^d$ that enclose p in their interior open ball. In a symmetric way, the upper halfspace, denoted as $\Phi(p)$ represents the spheres that do not enclose p in their interior.

In general, for a flat A in $\mathbb{E}^{d+1}$, we denote as A^* the polar of A with respect to Π:

$$A^* = \left\{ (x, \chi) \in \mathbb{E}^{d+1}, \forall a = (x_a, \chi_a) \in A, \frac{\chi + \chi_a}{2} = < x_a, x > \right\},$$

If $A \oplus B$ denotes the affine sum of two flats A and B, standard algebra shows that

$$(A \cap B)^* = A^* \oplus B^*. \tag{1}$$

Euclidean Voronoi diagram and Delaunay triangulation

Let $\mathcal{P}$ be a finite set of points in $\mathbb{E}^d$. For the sake of simplicity, we assume points to be in non-degenerate position. This is in fact not a restriction of our method, since we can always come down to this situation by using a symbolic perturbation scheme as in [18] (the paper describes the 3D case but the scheme is general).

The Euclidean Voronoi diagram $\mathrm{VD}_{\mathbb{E}}(\mathcal{P})$ of $\mathcal{P}$ is the partition of $\mathbb{E}^d$ into Voronoi cells $V_{\mathbb{E}}(p_i) = \{x \in \mathbb{E}^d \mid \forall p_j \in \mathcal{P}, \|x - p_i\| \leq \|x - p_j\|\}$. The Euclidean Delaunay triangulation $\mathrm{DT}_{\mathbb{E}}(\mathcal{P})$ is the geometric dual of the Voronoi diagram. For further reading on these extensively studied data structures, see for instance [13, 9, 2, 3].

Each cell $V_{\mathbb{E}}(p_i)$ of the Voronoi diagram can be interpreted as the set of centers of spheres passing through p_i and enclosing no point of $\mathcal{P}$. The set of *empty* spheres, ie. spheres that do not enclose any point of $\mathcal{P}$, is mapped by ϕ in the space of spheres to the intersection of the upper half spaces $\Phi(p)$ of $\mathbb{E}^{d+1}$, $p \in \mathcal{P}$, as defined above. The boundary of this intersection is a convex polyhedron $U_{\mathcal{P}}$, whose facets are tangent to Π. The correspondence between $\mathrm{VD}_{\mathbb{E}}(\mathcal{P})$ and $U_{\mathcal{P}}$ is a different way of seeing the well-known duality between Voronoi diagrams and arrangements [19]:

Proposition 1 ([15]) *The Voronoi diagram $VD_{\mathbb{E}}(\mathcal{P})$ is the cell complex of dimension d in $\mathbb{E}^d$ obtained by vertically projecting the polyhedron $U_{\mathcal{P}}$ onto $\mathbb{E}^d$.*

If σ is a k-simplex of $\mathrm{DT}_{\mathbb{E}}(\mathcal{P})$, we denote as $\mathcal{P}_\sigma$ the set of its vertices. The dual of σ is a $(d-k)$-face of $\mathrm{VD}_{\mathbb{E}}(\mathcal{P})$, which is the vertical projection of a $(d-k)$-face u_σ of $U_{\mathcal{P}}$. Any point in u_σ is the image by ϕ of the center of a sphere passing through the vertices of σ. Thus, u_σ is a convex polyhedron included in the $(d-k)$-flat $\bigcap_{p\in\mathcal{P}_\sigma} \phi(p)^*$ that is the intersection of the hyperplanes dual to $\phi(p)$ for all vertices p of σ.

The k-simplex σ is incident to m $(k+1)$-simplices $\tau_0, \tau_1, \ldots, \tau_{m-1}$ of $\mathrm{DT}_{\mathbb{E}}(\mathcal{P})$. The set of vertices of a simplex τ_i of this family is $\mathcal{P}_{\tau_i} = \mathcal{P}_\sigma \cup \{p_i\}$, for some point $p_i \in \mathcal{P} \setminus \mathcal{P}_\sigma$. The duals of these simplices τ_i determine the boundary of u_σ on the $(d-k)$-flat $\bigcap_{p\in\mathcal{P}_\sigma} \phi(p)^*$. To summarize:

$$u_\sigma = \bigcap_{p\in\mathcal{P}_\sigma} \phi(p)^* \bigcap \bigcap_{0\leq i<m} \Phi(p_i). \tag{2}$$

3 The Poincaré ball model of the hyperbolic space

The hyperbolic space $\mathbb{H}^d$ [5, Chapter 19] [33, 36] can be represented by several widely used models. There are transformations between these models, as recalled in [28, 34].

In the Poincaré ball model, the d-dimensional hyperbolic space $\mathbb{H}^d$ is represented as the open unit ball $\mathcal{B} = \{x \in \mathbb{E}^d : \|x\| < 1\}$. The points on the boundary of $\mathcal{B}$ are the *points at infinity*. The set of such points is $\mathcal{H}_\infty = \{x \in \mathbb{E}^d : \|x\| = 1\}$. Hyperbolic lines, or geodesics, are represented either as arcs of Euclidean circles orthogonal to $\mathcal{H}_\infty$ or as diameters of $\mathcal{B}$. See Figure 2 for an illustration in 2D.

The Poincaré ball model of $\mathbb{H}^d$ can be embedded into $\mathbb{E}^{d+1}$ by identifying it with the open unit d-disk $\chi = 0$, $\|x\| < 1$.

In the space of spheres, the set of points at infinity $\mathcal{H}_\infty$ (ie. the unit sphere in $\mathbb{E}^d$) is mapped to the point

$$\phi(\mathcal{H}_\infty) = (0, \ldots, 0, -1).$$

Its polar hyperplane is

$$\pi_\infty = \phi(\mathcal{H}_\infty)^* : \ \chi = 1.$$

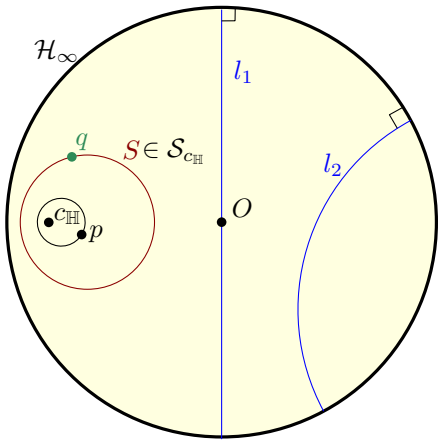

Figure 2: The Poincaré disk model of $\mathbb{H}^2$: hyperbolic lines l_1, l_2, hyperbolic circle S with center $c_\mathbb{H}$.

$\mathbb{H}^d$ is mapped to the part of the hyperboloid Π that lies below π_∞. For a point $x \in \mathcal{H}_\infty$, the hyperplane $\phi(x)^*$ is tangent to Π and passes through $\phi(\mathcal{H}_\infty)$.

Hyperbolic spheres are Euclidean spheres contained in $\mathcal{B}$, but the center of a hyperbolic sphere usually does not coincide with its Euclidean center. Let us consider the pencil of spheres determined by $\mathcal{H}_\infty$ and a point $c_\mathbb{H} \in \mathcal{B}$ considered as a sphere of radius 0. Those spheres of the pencil that are contained in $\mathcal{B}$ are the hyperbolic spheres centered at $c_\mathbb{H}$. We denote them by $\mathcal{S}_{c_\mathbb{H}}$. They represent a collection of nested spheres growing from $c_\mathbb{H}$ to $\mathcal{B}$. In the space of spheres $\mathbb{E}^{d+1}$, $\phi(\mathcal{S}_{c_\mathbb{H}})$ is the half-open line segment $[\phi(c_\mathbb{H}), \phi(\mathcal{H}_\infty))$.

A point p is closer than point q to point $c_\mathbb{H}$ for the hyperbolic distance if the sphere of $\mathcal{S}_{c_\mathbb{H}}$ that passes through p is inside the sphere of $\mathcal{S}_{c_\mathbb{H}}$ that passes through q (Figure 2). Note that we do not need to consider the explicit expression of the hyperbolic distance. See [4] for its more complete description.

The intersection of the upper half spaces of $\mathbb{E}^{d+1}$ limited by the hyperplanes $\phi(x)^*$, $x \in \mathcal{H}_\infty$ forms the cone C with apex $\phi(\mathcal{H}_\infty)$ tangent to Π (see Figure 3). C represents the set of Euclidean spheres that do not intersect $\mathcal{H}_\infty$. The set of hyperbolic spheres is the set of Euclidean spheres inside $\mathcal{B}$. In the space of spheres, it is mapped to the open subset C_Π of C that lies below π_∞ and below Π. C_Π can also be seen as $\cup_{x \in \mathcal{B}} \phi(\mathcal{S}_x)$.

Let $S \subset \mathcal{B}$ a hyperbolic sphere mapped to $\phi(S) \in C_\Pi$ in the space of spheres. We denote as ψ_Π the *central projection* onto Π centered at $\phi(\mathcal{H}_\infty)$: $\psi_\Pi(\phi(S))$ is the intersection of line $(\phi(\mathcal{H}_\infty)\phi(S))$ with Π. This intersection point is in fact the projection by ϕ on Π of the hyperbolic center $c_\mathbb{H}$ of S. Note that hyperbolic spheres are the only spheres on which this central projection is defined: for a Euclidean sphere S that is not contained in $\mathcal{B}$, the line $(\phi(\mathcal{H}_\infty)\phi(S))$ does not intersect Π.

We denote as ψ_{π_∞} the central projection centered at $\phi(\mathcal{H}_\infty)$ onto π_∞.

4 Computing the hyperbolic Delaunay complex

Let $\mathcal{P}$ be a finite set of points in $\mathbb{H}^d$, represented in the Poincaré ball model. The hyperbolic Voronoi diagram $\mathrm{VD}_\mathbb{H}(\mathcal{P})$ is defined as its Euclidean counterparts, replacing the Euclidean dis-

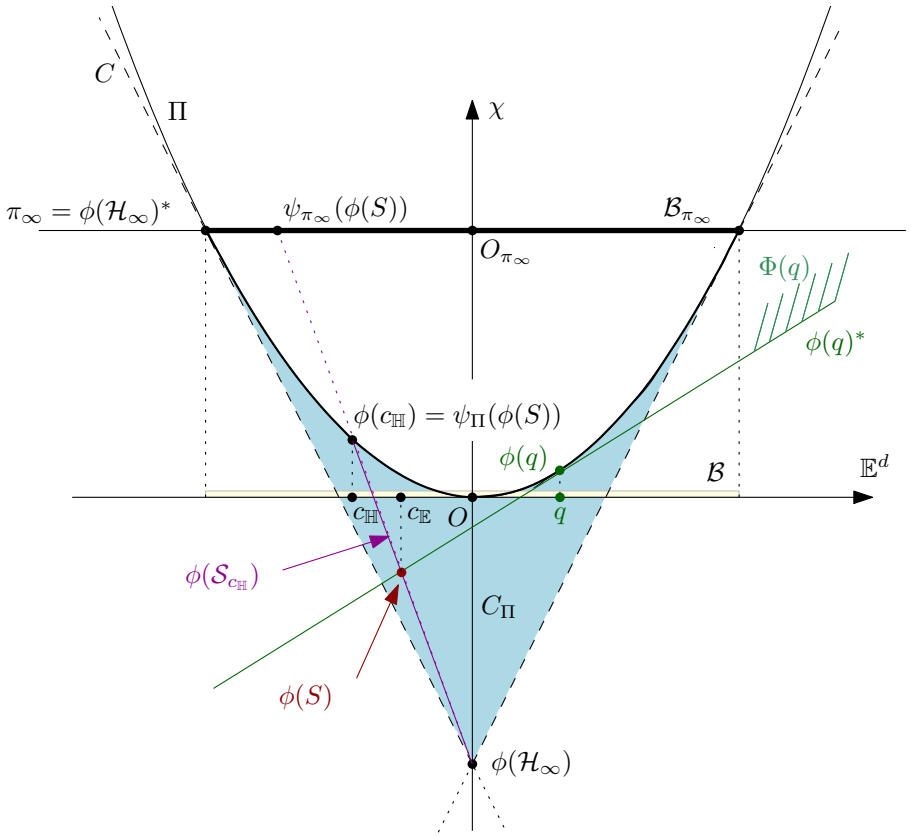

Figure 3: The Poincaré ball model of $\mathbb{H}^d$ in the space of spheres. $q \in S$, $c_\mathbb{E}$ is the Euclidean center of S, $c_\mathbb{H}$ is its hyperbolic center.

tance by the hyperbolic distance.

Let us take a point x in the cell $V_\mathbb{H}(p_i)$ of p in $\mathrm{VD}_\mathbb{H}(\mathcal{P})$. x is closer to p_i than to any other point in $\mathcal{P}$ for the hyperbolic distance. As already noted, we can avoid considering the hyperbolic distance explicitly, and express this proximity property in other words: a sphere of the pencil generated by the sphere of null radius x and $\mathcal{H}_\infty$, and growing from x to the sphere $\mathcal{H}_\infty$, meets p_i before meeting any other point of $\mathcal{P}$. This illustrates the fact that for every point x in $V_\mathbb{H}(p_i)$ there exists a unique sphere S hyperbolically centered at x passing through p_i and enclosing no point of $\mathcal{P}$.

A simplex σ is an element of the *hyperbolic Delaunay complex* $\mathrm{DT}_\mathbb{H}(\mathcal{P})$ *iff* there exists a point $c \in \mathbb{H}^d$ that is the hyperbolic center of a hyperbolic sphere (ie. a Euclidean sphere contained in $\mathcal{B}$) passing through the vertices of σ and enclosing no point of $\mathcal{P}$ in its open interior ball.

An example, drawn with our implementation (see Section 6), is shown on Figure 4.

Note that some k-simplices in the hyperbolic Delaunay complex may have no $(k+1)$-simplices in the complex incident to them. This is the reason why we don't call $\mathrm{DT}_\mathbb{H}(\mathcal{P})$ a triangulation. $\mathrm{DT}_\mathbb{H}(\mathcal{P})$ is still a simplicial complex.

Let us prove a property of $\mathrm{DT}_\mathbb{H}(\mathcal{P})$, which will not be used in the algorithm, but which is still interesting in itself.

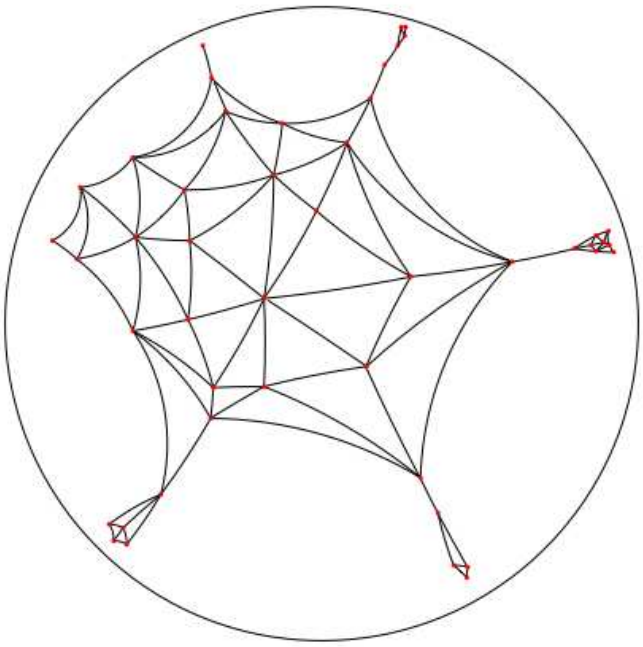

Figure 4: Hyperbolic Delaunay complex.

Proposition 2 *The Delaunay complex $DT_{\mathbb{H}}(\mathcal{P})$ is connected.*

The proof is a direct consequence of the following Lemma.

Lemma 3 *Let $\mathcal{P}$ be partitioned into a set R of red points and a set B of blue points. Then there exist two points $p_r \in R$ and $p_b \in B$, and an empty sphere S_{pq} passing through p_r and p_b that is contained in $\mathcal{B}$.*

Proof. Let us first construct a sphere S_0 centered at the origin O by starting from the unit ball $\mathcal{B}$ and reducing its radius until it contains points of only one color. Without loss of generality, S_0 contains only blue points. Let p_r be the red point though which S_0 passes.

Then we construct another sphere S_{pq}, by starting from S_0 and reducing the radius, while keeping the sphere in the pencil of spheres through p_r and tangent to S_0, until it is empty. Let p_b be the blue point though which S_{pq} passes.

We have constructed a sphere S_{pq} whose open interior ball is empty, that passes though p_r and p_b, and that is contained in $\mathcal{B}$. □

The existence of the sphere shows that for any partition of $\mathcal{P}$ into two sets of points, there is an edge of the hyperbolic Delaunay complex between these two sets, which proves Proposition 2.

The correspondence between $\mathrm{VD}_{\mathbb{H}}(\mathcal{P})$ and $\mathrm{VD}_{\mathbb{E}}(\mathcal{P})$ can be seen as follows, using the central projection ψ_Π (see Section 3). Let $f_{\mathbb{E}}$ be a k-face of $\mathrm{VD}_{\mathbb{E}}(\mathcal{P})$, ie. the set of Euclidean centers of empty spheres passing through a subset $\mathcal{P}_f$ of $d+1-k$ points of $\mathcal{P}$. By Proposition 1, $f_{\mathbb{E}}$ is the vertical projection of a k-face f_U of $U_{\mathcal{P}}$. Let $c_{\mathbb{E}}$ be a point of $f_{\mathbb{E}}$, i.e. the Euclidean center

of an empty sphere $S \subset \mathbb{E}^d$ passing through $\mathcal{P}_f$. If S is contained in $\mathcal{B}$, the point obtained by centrally projecting $\phi(S) \in f_U$ to Π from $\phi(\mathcal{H}_\infty)$ is $\psi_\Pi(\phi(S))$, which projects vertically onto the hyperbolic center $c_\mathbb{H}$ of S (see Figure 3). This can be summarized as:

Proposition 4 ([15]) *The hyperbolic Voronoi diagram $VD_\mathbb{H}(\mathcal{P})$ can be obtained by centrally projecting from $\phi(\mathcal{H}_\infty)$ the part of the polyhedron $U_\mathcal{P}$ lying in C_Π to the paraboloid Π, and projecting the result vertically onto $\mathbb{E}^d$.*

As a consequence, $DT_\mathbb{H}(\mathcal{P})$ is a subcomplex of $DT_\mathbb{E}(\mathcal{P})$. It consists of faces of $DT_\mathbb{E}(\mathcal{P})$ that admit at least one empty ball passing though its vertices and included in $\mathcal{B}$.

The computation of $\mathrm{DT}_\mathbb{H}(\mathcal{P})$ thus consists of the following two steps:

- Compute the Euclidean Delaunay triangulation $\mathrm{DT}_\mathbb{E}(\mathcal{P})$,
- Extract from $\mathrm{DT}_\mathbb{E}(\mathcal{P})$ the simplices that also belong to $\mathrm{DT}_\mathbb{H}(\mathcal{P})$.

The rest of this section is devoted to showing how this extraction step can be performed. We first describe variants of this general scheme. The predicate that tests whether a given simplex of $\mathrm{DT}_\mathbb{E}(\mathcal{P})$ is also in $\mathrm{DT}_\mathbb{H}(\mathcal{P})$ is denoted as *is_hyperbolic* and will be detailed in Section 4.2.

4.1 Extracting $\mathrm{DT}_\mathbb{H}(\mathcal{P})$ from $\mathrm{DT}_\mathbb{E}(\mathcal{P})$: algorithms

We give several variants of the extraction scheme. The basic one closely follows what was just presented. The second is an improvement that allows to test a smaller number of simplices. Both are static, ie., they first compute the whole Euclidean triangulation before performing the extraction. The third is dynamic: it allows to add a point and to update the hyperbolic Delaunay complex while the Euclidean Delaunay triangulation is updated.

Basic algorithm

Let us first remark that, if a simplex of $\mathrm{DT}_\mathbb{E}(\mathcal{P})$ also belongs to the hyperbolic Delaunay complex $\mathrm{DT}_\mathbb{H}(\mathcal{P})$, then all its faces also belong to $\mathrm{DT}_\mathbb{H}(\mathcal{P})$. Extracting $\mathrm{DT}_\mathbb{H}(\mathcal{P})$ from $\mathrm{DT}_\mathbb{E}(\mathcal{P})$ can be done by examining simplices by decreasing dimensions, starting from d-simplices. The extraction consists in simply marking each k-simplex of $\mathrm{DT}_\mathbb{E}(\mathcal{P})$, $k = 1, \ldots, d$ as "hyperbolic" or "non-hyperbolic".

For each dimension k, we maintain a dictionary D_k of simplices to be examined. The dictionary D_d initially contains all d-simplices of $\mathrm{DT}_\mathbb{E}(\mathcal{P})$, other dictionaries are empty. The algorithm proceeds by decreasing dimensions, starting at $k = d$.

For each k, $d \geq k \geq 1$;
  while $D_k \neq \emptyset$ we pop the first k-simplex σ of $\mathrm{DT}_\mathbb{E}(\mathcal{P})$ out of D_k;
    If it is marked already, don't do anything;
    If it is not marked yet, we test whether it is a simplex of $\mathrm{DT}_\mathbb{H}(\mathcal{P})$;
      If yes, we mark σ as "hyperbolic", as well as all its faces of all dimensions i from $k-1$ down to 1;
      If not, we mark σ as "non-hyperbolic". Its $(k-1)$-faces are not examined. We insert them into D_{k-1};
  end while;
end for.

Anticipating on Section 4.2, in which it will be clear that predicate *is_hyperbolic* can be evaluated with constant complexity, we get:

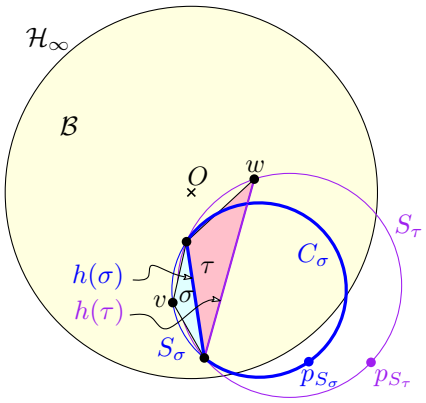

Figure 5: Proof of Prop 6.

Proposition 5 *The hyperbolic Delaunay complex of n points in the Poincare ball model $\mathbb{H}^d$ can be computed in time $\Theta\left(n \log n + n^{\lceil d/2 \rceil}\right)$.*

Improved extraction scheme

This improved scheme does not reduce the theoretical complexity given in Proposition 5, but it makes the extraction "output-sentitive" in some way: it is not sensitive to the number of simplices in the result $\mathrm{DT}_{\mathbb{H}}(\mathcal{P})$, but to the number of simplices that are *not* in the result, ie., to the size of $\mathrm{DT}_{\mathbb{E}}(\mathcal{P}) \setminus \mathrm{DT}_{\mathbb{H}}(\mathcal{P})$.

We consider that the Euclidean space $\mathbb{E}^d$ is compactified to a topological sphere by the addition of a point at infinity. This point at infinity can be linked to all simplices of the convex hull of $\mathcal{P}$. After adding these infinite simplices to it, the Euclidean triangulation $\mathrm{DT}_{\mathbb{E}}(\mathcal{P})$ becomes a triangulation of a combinatorial sphere.

Proposition 6 *The graph G whose nodes are the d-simplices of $DT_{\mathbb{E}}(\mathcal{P}) \setminus DT_{\mathbb{H}}(\mathcal{P})$ and the infinite d-simplices of $DT_{\mathbb{E}}(\mathcal{P})$, and whose arcs are adjacency relations through facets in $DT_{\mathbb{E}}(\mathcal{P})$, is connected.*

Proof. We first remark that the infinite simplices of $\mathrm{DT}_{\mathbb{E}}(\mathcal{P})$ form the set of all simplices that are adjacent to the infinite vertex, so, their graph is connected.

Let σ be a finite d-simplex of $\mathrm{DT}_{\mathbb{E}}(\mathcal{P})$ that is not in $\mathrm{DT}_{\mathbb{H}}(\mathcal{P})$. The sphere S_σ circumscribing σ intersects $\mathcal{H}_\infty$. More precisely, among the d spherical caps on S_σ that are limited by the supporting (Euclidean) hyperplanes of the facets of σ and that do not contain any vertex of σ, at least one cap intersects $\mathcal{H}_\infty$. If there are several such caps, we choose one that contains the point p_{S_σ} of S_σ that is the farthest to O.

Let us call C_σ such a cap and $h(\sigma)$ the corresponding facet of σ (See Figure 5). Any sphere S' passing though the vertices of $h(\sigma)$ either encloses the vertex v of σ opposite to $h(\sigma)$, or intersects $\mathcal{H}_\infty$. Thus, the $(d-1)$-simplex $h(\sigma)$ does not belong to $\mathrm{DT}_{\mathbb{H}}(\mathcal{P})$. Moreover, when S' does not enclose v, it encloses p_{S_σ}, and its point $p_{S'}$ farthest to O is such that $\|Op_{S'}\| > \|Op_{S_\sigma}\|$.

Let τ be the neighbor of σ through $h(\sigma)$ in $\mathrm{DT}_{\mathbb{E}}(\mathcal{P})$ and w the vertex of τ that is not in $h(\sigma)$. Observe that $\tau \notin \mathrm{DT}_{\mathbb{H}}(\mathcal{P})$; otherwise $h(\sigma)$ would have been in $\mathrm{DT}_{\mathbb{H}}(\mathcal{P})$ since $h(\sigma)$ is a face of τ. Then, observe that $\|Op_{S_\tau}\| > \|Op_{S_\sigma}\|$. A path of d-simplices can be constructed in graph G, using adjacency relations, starting at σ and ending at an infinite simplex, by choosing at each step the adjacent simplex through $h(\sigma)$. This path traverses only simplices of $\mathrm{DT}_{\mathbb{E}}(\mathcal{P}) \setminus \mathrm{DT}_{\mathbb{H}}(\mathcal{P})$. □

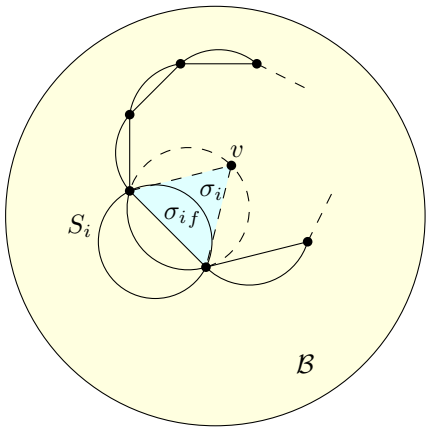

Figure 6: Proof of Lemma 8.

Corollary 7 *If $d = 2$, there is a bijection h between non-hyperbolic triangles and non-hyperbolic edges.*

Proof. In dimension 2, the definition of $h(\sigma)$ appearing in the proof of Proposition 6 does not involve any choice of a good spherical cap, since in two dimensions the three caps are disjoint and only one intersects $\mathcal{H}_\infty$. The mapping h has been proved to be injective. It remains to prove that any edge $e \in \mathrm{DT}_{\mathbb{E}}(\mathcal{P}) \setminus \mathrm{DT}_{\mathbb{H}}(\mathcal{P})$ is the image by h of a triangle σ. Let S be a circle circumscribing e. S intersects $\mathcal{H}_\infty$, otherwise $e \in \mathrm{DT}_{\mathbb{H}}(\mathcal{P})$. Then we consider circles of the pencil of circles passing through the vertices of e, starting from from S, and going in the direction that decreases the intersection with $\mathcal{H}_\infty$, until we find a vertex v of $\mathcal{P}$. Vertex v and edge e form the Euclidean Delaunay triangle σ such that $h(\sigma) = f$. □

The improved version of the extraction algorithm consists in "digging" $\mathrm{DT}_{\mathbb{E}}(\mathcal{P})$: its starts from the infinite d-simplices of $\mathrm{DT}_{\mathbb{E}}(\mathcal{P})$, and recursively traverses G using adjacency relations. The recursive traversal stops digging as soon as it can only reach d-simplices on which *is_hyperbolic* is true. During the traversal, faces of all d-simplices of G are tested against *is_hyperbolic* and marked accordingly as in the basic algorithm.

Dynamic variant

Let us quickly recall the following definitions: The *star* $St_X(v)$ of a vertex v in a simplicial complex X is defined to be the subcomplex consisting of all cofaces of v, ie., all the simplices of X that contain v and their faces. The *link* $Lk_X(v)$ of v is the subcomplex of X consisting of all faces of $St(v)$ that do not contain v.

Lemma 8 *If all the $(d-1)$-simplices of $Lk_{DT_{\mathbb{E}(\mathcal{P})}}(v)$ belong to $DT_{\mathbb{H}}(\mathcal{P})$, then $St_{DT_{\mathbb{E}(\mathcal{P})}}(v)$ is a subcomplex of $DT_{\mathbb{H}}(\mathcal{P})$.*

Proof. Let $\sigma_0, \sigma_1, \ldots, \sigma_{m-1}$ be the d-simplices in $St_{\mathrm{DT}_{\mathbb{E}(\mathcal{P})}}(v)$, and $\sigma_{if}, 0 \leq i < m$ be the facet of σ_i opposite to v. The hypothesis means that there is an empty ball B_i included in $\mathcal{B}$ whose boundary S_i passes through the vertices of σ_{if} (See Figure 6). The circumscribing ball of each $\sigma_j, 0 \leq j < m$, is included in the union $\cup_{i=0}^{m-1}(B_i \cup \sigma_i)$, so, it is also included in $\mathcal{B}$. □

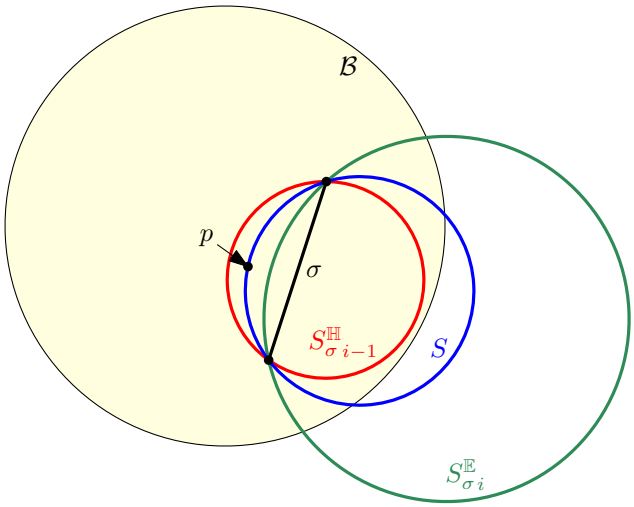

Figure 7: Proof of Lemma 9.

This variant consists in using a dynamic algorithm, allowing the Euclidean Delaunay triangulation to be updated at each insertion of a new point. At the same time, we can update the hyperbolic complex in an efficient way, by updating the marks "hyperbolic" or "non-hyperbolic". Let p be the i^{th} point, and $\mathcal{P}_{i-1}$ be the set of $i-1$ points inserted before. The insertion of p removes a set of d-simplices from $\mathrm{DT}_{\mathbb{E}}(\mathcal{P}_{i-1})$, whose union forms a topological ball, and whose boundary is the link of p in $\mathrm{DT}_{\mathbb{E}}(\mathcal{P}_{i-1}\cup\{p\})$. These simplices are replaced in by simplices of the star of p in $\mathrm{DT}_{\mathbb{E}}(\mathcal{P}_{i-1}\cup\{p\})$. Let us consider the set Σ of d-simplices of $\mathrm{DT}_{\mathbb{E}}(\mathcal{P}_{i-1}\cup\{p\})$ that lie outside this topological ball and that are adjacent through a facet to some d-simplex in this star.

- If, for any d-simplex $\sigma\in\Sigma$, σ is an element of in $\mathrm{DT}_{\mathbb{H}}(\mathcal{P}_{i-1})$, ie., if it is marked as hyperbolic in $\mathrm{DT}_{\mathbb{E}}(\mathcal{P}_{i-1})$, then all simplices in the link of p are hyperbolic, since they are facets of hyperbolic simplices. So, by Lemma 8, all new simplices of $\mathrm{DT}_{\mathbb{E}}(\mathcal{P}_{i-1}\cup\{p\})$ created by the insertion of p are in $\mathrm{DT}_{\mathbb{H}}(\mathcal{P}_{i-1}\cup\{p\})$. In such a good case, there is no need to run *is_hyperbolic* on any simplex.
- Otherwise, we check new simplices and their faces with *is_hyperbolic*, starting from d-simplices and going down in dimensions, as in the basic algorithm. Note that faces of new simplices must be checked, even if they are not new, since their mark may need to be updated.

To show the correctness of this algorithm, it remains to show the following:

Lemma 9 *A k-simplex σ that was in $DT_{\mathbb{H}}(\mathcal{P}_{i-1})$ and stays in $DT_{\mathbb{E}}(\mathcal{P}_{i-1}\cup\{p\})$ can become non-hyperbolic after the insertion of p only if σ is in the link of p in $DT_{\mathbb{E}}(\mathcal{P}_{i-1}\cup\{p\})$.*

Proof. Let σ be a k-simplex of $\mathrm{DT}_{\mathbb{H}}(\mathcal{P}_{i-1})$ that stays in $\mathrm{DT}_{\mathbb{E}}(\mathcal{P}_{i-1}\cup\{p\})$. Let us assume that σ does not belong to $\mathrm{DT}_{\mathbb{H}}(\mathcal{P}_{i-1}\cup\{p\})$. Then there was at least one empty sphere $S^{\mathbb{H}}_{\sigma\, i-1}$ passing through the vertices of σ and included in $\mathcal{B}$ before p was inserted, and there is no such sphere any more afterwards. So, $S^{\mathbb{H}}_{\sigma\, i-1}$ encloses p in its open interior ball (see Figure 7). The simplex σ

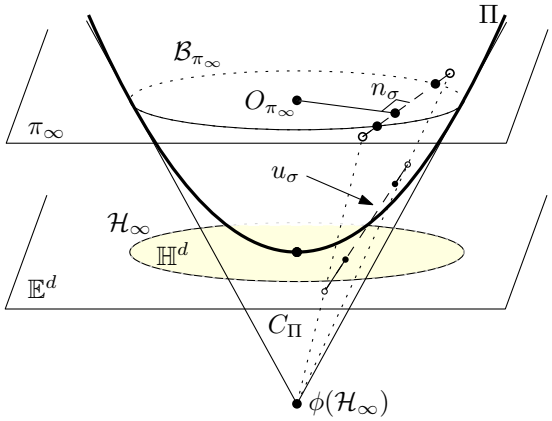

Figure 8: Condition for a simplex σ of $\mathrm{DT}_\mathbb{E}(\mathcal{P})$ to be a simplex of $\mathrm{DT}_\mathbb{H}(\mathcal{P})$.

stays in $\mathrm{DT}_\mathbb{E}(\mathcal{P}_{i-1}\cup\{p\})$, so, there is at least one empty (not containing any point of $\mathcal{P}_{i-1}\cup\{p\}$) sphere $S^\mathbb{E}_{\sigma\, i}$ passing though the vertices of σ.

Let us consider the pencil of spheres generated by $S^\mathbb{H}_{\sigma\, i-1}$ and $S^\mathbb{E}_{\sigma\, i}$. There is a sphere in this pencil that passes through p. This sphere S is included in the union of the two balls interior to $S^\mathbb{H}_{\sigma\, i-1}$ and $S^\mathbb{E}_{\sigma i}$, so, it is is empty. S passes though all the vertices of $\sigma\cup\{p\}$. So, $\sigma\cup\{p\}$ is a $(k+1)$-simplex in $\mathrm{DT}_\mathbb{E}(\mathcal{P}_{i-1}\cup\{p\})$, and σ is an element of the link of p in this triangulation. □

So, simplices outside the link of p in $\mathrm{DT}_\mathbb{E}(\mathcal{P}_{i-1}\cup\{p\})$ don't need to be tested.

Altogether, this discussion shows that the dynamic variant to compute the hyperbolic Delaunay triangulation has the same complexity as the dynamic algorithm to compute the Euclidean triangulation. Using an appropriate point location data structure [14], we get:

Proposition 10 *The dynamic variant has optimal randomized worst-case time complexity* $O\left(n^{\lceil\frac{d}{2}\rceil}+n\log n\right)$ *and space complexity* $O\left(n^{\lceil\frac{d}{2}\rceil}\right)$.

4.2 Extracting $\mathrm{DT}_\mathbb{H}(\mathcal{P})$ from $\mathrm{DT}_\mathbb{E}(\mathcal{P})$: predicate

Let us now explain the test *is_hyperbolic*, which checks whether a simplex of $\mathrm{DT}_\mathbb{E}(\mathcal{P})$ is in $\mathrm{DT}_\mathbb{H}(\mathcal{P})$. Let observe right now that this predicate has no degenerate case: as mentioned in Section 3 (page 6), hyperbolic spheres are Euclidean spheres contained in the *open* ball $\mathcal{B}$. The only candidate for a degenerate case would be the limit case when the only empty sphere passing through the vertices of a given simplex is *tangent* to $\partial\mathcal{B}=\mathcal{H}_\infty$. Then the simplex is just not hyperbolic, and the case is in fact not degenerate.

We first look at d-simplices. Let σ be a d-simplex of $\mathrm{DT}_\mathbb{E}(\mathcal{P})$, dual to a Voronoi vertex, projected from the vertex u_σ of $U_\mathcal{P}$ in $\mathbb{E}^{d+1}$. u_σ is the image by ϕ of the (empty) sphere circumscribing σ. From Section 3, σ is a d-simplex of $\mathrm{DT}_\mathbb{H}(\mathcal{P})$ *iff* u_σ lies in C_Π. Since $\mathcal{P}\subset\mathcal{B}$, the circumscribing sphere of σ cannot completely lie outside $\mathcal{B}$, so, this equivalence can be rewritten as: σ is a d-simplex of $\mathrm{DT}_\mathbb{H}(\mathcal{P})$ *iff* u_σ lies in C.

For a general dimension k, the discussion at the end of Section 3 straightforwardly shows that the following conditions are equivalent:

1. the k-simplex $\sigma, k\le d$ of $\mathrm{DT}_\mathbb{E}(\mathcal{P})$ is a simplex of $\mathrm{DT}_\mathbb{H}(\mathcal{P})$

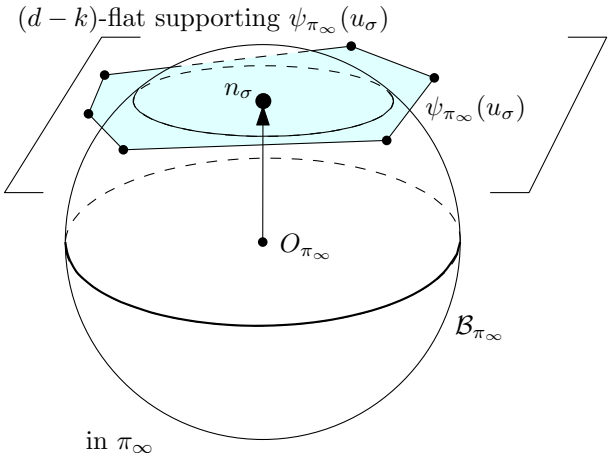

Figure 9: The central projection of u_σ on π_∞ intersects the open unit d-ball $\mathcal{B}_{\pi_\infty}$ in π_∞.

2. u_σ intersects C
3. $\psi_\Pi(u_\sigma) \neq \emptyset$
4. $\psi_{\pi_\infty}(u_\sigma)$ intersects the open unit d-ball $\mathcal{B}_{\pi_\infty}$ of π_∞.

See Figure 8 for an illustration.

If σ is a k-simplex of $\mathrm{DT}_{\mathbb{H}}(\mathcal{P})$ whose incident $(k+1)$-simplices do not belong to $\mathrm{DT}_{\mathbb{H}}(\mathcal{P})$, the central projection $\psi_{\pi_\infty}(u_\sigma)$ of u_σ onto π_∞ is a convex $(d-k)$-polyhedron whose facets lie outside the unit d-ball $\mathcal{B}_{\pi_\infty}$ in π_∞ (See Figure 9). The polyhedron $\psi_{\pi_\infty}(u_\sigma)$ intersects $\mathcal{B}_{\pi_\infty}$, but its boundary does not intersect $\mathcal{B}_{\pi_\infty}$, so, the whole intersection of the supporting flat of $\psi_{\pi_\infty}(u_\sigma)$ with $\mathcal{B}_{\pi_\infty}$ is contained in $\psi_{\pi_\infty}(u_\sigma)$. So, it is sufficient to test any well chosen point in the intersection of the supporting flat and the ball $\mathcal{B}_{\pi_\infty}$. In hyperplane π_∞, let n_σ be the point of the supporting $(d-k)$-flat of $\psi_{\pi_\infty}(u_\sigma)$ that is the nearest to the origin O_{π_∞} of $\mathcal{B}_{\pi_\infty}$. Predicate *is_hyperbolic* will check whether $\psi_{\pi_\infty}(u_\sigma)$ intersects $\mathcal{B}_{\pi_\infty}$, ie.,

$$\textit{is\_hyperbolic}(\sigma)$$
$$\Updownarrow$$
n_σ is contained in both the convex polyhedron $\psi_{\pi_\infty}(u_\sigma)$ and the ball $\mathcal{B}_{\pi_\infty}$.

5 Geometric proofs for algebraic aspects

In this section we first recall how the Euclidean Delaunay triangulation $\mathrm{DT}_{\mathbb{E}}(\mathcal{P})$ can be computed only using rational computations. Then we show in Section 5.2 that extracting the hyperbolic Delaunay complex $\mathrm{DT}_{\mathbb{H}}(\mathcal{P})$ from $\mathrm{DT}_{\mathbb{E}}(\mathcal{P})$ can also be performed only using rational computations. In Section 5.3, we consider the geometric embedding of $\mathrm{DT}_{\mathbb{H}}(\mathcal{P})$ in the Poincaré ball model. The algebraic aspects of the geometric embedding of $\mathrm{VD}_{\mathbb{H}}(\mathcal{P})$ are studied in Section 5.4.

We assume that the coordinates $(x_0, \ldots, x_{d-1})$ of each point x of $\mathcal{P}$ are rational.

5.1 Computing $\mathrm{DT}_{\mathbb{E}}(\mathcal{P})$

This section quickly recalls basic facts, we refer the reader to the mentioned literature for more details. Many standard algorithms have been proposed to compute $\mathrm{DT}_{\mathbb{E}}(\mathcal{P})$. The CGAL library

[1] offers an efficient implementation in 2D and 3D [38, 30], based on the incremental construction first proposed by Bowyer [10] and Watson [35]. Several options are proposed for point location, using either some walking strategy [17] or a hierarchical data structure [14].

The robustness of the implementation against arithmetic issues is ensured by following the exact geometric paradigm [37]. The computation of the combinatorial structure underlying $\mathrm{DT}_{\mathbb{E}}(\mathcal{P})$ only relies on the evaluation of two predicates.

The predicate *orientation*$(p_0, p_1, \ldots, p_d)$ decides the orientation of $d+1$ points, and boils down to the sign of the determinant:

$$\begin{vmatrix} p_{0_0} & p_{0_1} & \cdots & p_{0_{d-1}} & 1 \\ p_{1_0} & p_{1_1} & \cdots & p_{1_{d-1}} & 1 \\ \vdots & \vdots & \vdots & \vdots & \vdots \\ p_{d_0} & p_{d_1} & \cdots & p_{d_{d-1}} & 1 \end{vmatrix}$$

The predicate *in_sphere*$(p_0, p_1, .., p_d, q)$ decides whether q lies in the open interior ball of the sphere passing through the $d+1$ first points. If we assume that these $d+1$ first points are positively oriented, then the predicate is given by the sign of the determinant:

$$\begin{vmatrix} p_{0_0} & p_{0_1} & \cdots & p_{0_{d-1}} & \|p_0\|^2 & 1 \\ p_{1_0} & p_{1_1} & \cdots & p_{1_{d-1}} & \|p_1\|^2 & 1 \\ \vdots & \vdots & \vdots & \vdots & \vdots & \vdots \\ p_{d_0} & p_{d_1} & \cdots & p_{d_{d-1}} & \|p_d\|^2 & 1 \\ q_0 & q_1 & \cdots & q_{d-1} & \|q\|^2 & 1 \end{vmatrix},$$

which is in fact exactly the orientation predicate of $(\phi(p_0), \phi(p_1), \ldots, \phi(p_d), \phi(q))$ in the space of spheres.

Only rational operations are needed to evaluate these signs of polynomial expressions. The computation is made both exact and fast by using filtered exact computations [16].

5.2 Extracting $\mathrm{DT}_{\mathbb{H}}(\mathcal{P})$ from $\mathrm{DT}_{\mathbb{E}}(\mathcal{P})$

Lemma 11 *Each rational point of $\mathbb{E}^{d+1}$ is projected by ψ_{π_∞} on π_∞ to a rational point.*

Proof. A point $(c, \chi) \in \mathbb{E}^{d+1}$ is projected to π_∞ following the line through $\phi(\mathcal{H}_\infty)$ to point $(x, 1)$, $x \in \mathbb{E}^d$, such that

$$x = \frac{2}{1+\chi} \cdot c.$$

Note that $1+\chi$ is the power product of the unit sphere $\mathcal{H}_\infty$ and the sphere S such that $\phi(S) = (c, \chi)$. □

Lemma 12 *The sphere S circumscribing a d-simplex σ whose vertices are rational points is mapped by ϕ to a rational point.*

Proof. $\phi(S) = \bigcap_{p \in \mathcal{P}_\sigma} \phi(p)^*$. Each $\phi(p)^*$ is a rational hyperplane of $\mathbb{E}^{d+1}$, so, the intersection is rational. □

Let us remark that a sphere $S \subset \mathbb{E}^d$ has rational Euclidean circumcenter and squared radius *iff* its associated point $\phi(S)$ in the space of spheres has rational coordinates.

The equation of cone C in $\mathbb{E}^{d+1}$ is given as follows

$$(x, \chi) \in C \iff \|x\|^2 - \left(\frac{1+\chi}{2}\right)^2 < 0. \tag{3}$$

Proposition 13 *The evaluation of the predicate* is_hyperbolic*, which tests whether a k-simplex of $DT_{\mathbb{E}}(\mathcal{P})$ belongs to $DT_{\mathbb{H}}(\mathcal{P})$, can be performed using rational computations only.*

Proof. Let σ be a k-simplex in $\mathrm{DT}_{\mathbb{E}}(\mathcal{P})$ and $\{\tau_i, 0 \leq i < m\}$ be the collection of its incident $(k+1)$-simplices in $\mathrm{DT}_{\mathbb{E}}(\mathcal{P})$. Then the corresponding $(d-k)$-face u_σ of $U_{\mathcal{P}}$ is given by Equation (2) (see Section 2). Thus, the construction of u_σ involves rational computations only. As shown by Lemma 11, the central projection $\psi_{\pi_\infty}(u_\sigma)$ of u_σ onto π_∞ is rational as well.

The projection n_σ of the origin O_{π_∞} onto the $(d-k)$-flat $\psi_{\pi_\infty}\left(\bigcap_{p\in\mathcal{P}_\sigma}\phi(p)^*\right)$ supporting $\psi_{\pi_\infty}(u_\sigma)$, as defined in Section 4.2, is given by the intersection of the normal to this $(d-k)$-flat passing through O_{π_∞} and itself, thus it is rational.

It remains to say that the test whether n_σ lies in the convex polyhedron given by Equation (2) boils down to *orientation* tests, and inclusion in $\mathcal{B}_{\pi_\infty}$ reduces to comparing its square distance to O_{π_∞} with 1. □

Altogether, Sections 5.1 and 5.2 show that the combinatorial structure of $\mathrm{DT}_{\mathbb{H}}(\mathcal{P})$ can be computed using only rational computations.

5.3 Computing the embedding of $\mathrm{DT}_{\mathbb{H}}(\mathcal{P})$ in the Poincaré ball

Let us now focus on the geometric embedding of $\mathrm{DT}_{\mathbb{H}}(\mathcal{P})$.

As already mentioned, a hyperplane (ie., a $(d-1)$-flat) in $\mathbb{H}^d$ is a portion of an Euclidean d-sphere. We say that the hyperplane is *rational* if the corresponding Euclidean sphere as a rational equation, ie., if its Euclidean center has rational coordinates and its squared Euclidean radius is rational, or equivalently, if it is mapped by ϕ to a rational point.

A k-flat in $\mathbb{H}^d$, for $k > 0$, is given by the intersection of $d-k$ hyperplanes. We say that the k-flat is *rational* if all these hyperplanes are rational. Then we inductively define a k-simplex to be *rational* if its supporting k-flat is rational and if its faces of dimensions $0, \ldots, k-1$ are rational.

Proposition 14 *In the Poincaré ball model, the geometric embedding of the hyperplane supporting any facet of $DT_{\mathbb{H}}(\mathcal{P})$ is rational.*

Proof. A facet of $\mathrm{DT}_{\mathbb{H}}(\mathcal{P})$ is a $(d-1)$-simplex supported by the hyperplane containing its vertices $p_0, p_1, \ldots, p_{d-1}$. This hyperplane is embedded in the Poincaré ball model as the Euclidean sphere S that passes through the p_i's and that is orthogonal to $\mathcal{H}_\infty$, ie.,

$$\phi(S) = \bigcap_{0\leq i<d-1} \phi(p_i)^* \bigcap \pi_\infty.$$

It is the intersection of hyperplanes of $\mathbb{E}^{d+1}$, which are all rational. □

Corollary 15 *The embedding of $DT_{\mathbb{H}}(\mathcal{P})$ is rational.*

Proof. By hypothesis on $\mathcal{P}$, each vertex of $\mathrm{DT}_{\mathbb{H}}(\mathcal{P})$ has rational coordinates. Each edge (1-simplex) of $\mathrm{DT}_{\mathbb{H}}(\mathcal{P})$ is supported by the intersection of $d-1$ hyperplanes, and its endpoints are rational vertices. The edge will be rational *iff* all hyperplanes are rational. In the same way, a k-simplex $\mathrm{DT}_{\mathbb{H}}(\mathcal{P})$, for any $k > 0$, will be rational *iff* all $d-k$ hyperplanes defining its supporting flat are rational. All considered hyperplanes are rational from Proposition 14, which concludes the proof. □

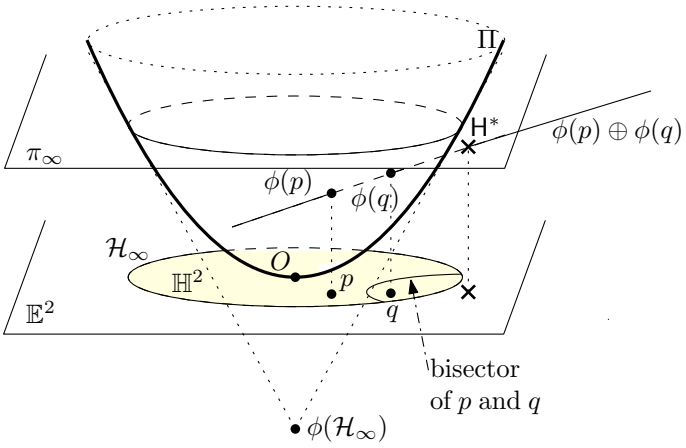

Figure 10: H^* is the image by ϕ of the bisector of p and q in $\mathbb{H}^2$.

5.4 Computing the embedding of $\mathrm{VD}_{\mathbb{H}}(\mathcal{P})$ in the Poincaré ball

Let us move on to the geometrical embedding of the hyperbolic Voronoi diagram $\mathrm{VD}_{\mathbb{H}}(\mathcal{P})$.

Proposition 16 *The bisector of two points of $\mathcal{P}$ is a hyperbolic hyperplane whose equation in $\mathbb{E}^d$ is rational.*

Proof. Let p and q be two points of $\mathcal{P}$. In the space of spheres, We are going to construct their hyperbolic bisector as the locus of hyperbolic centers of spheres passing through both of them.

The intersection $\phi(p)^* \cap \phi(q)^*$ is the $(d-1)$-flat in the space of spheres $\mathbb{E}^{d+1}$ that represent all spheres of $\mathbb{E}^d$ passing through p and q. By the construction explained earlier for hyperbolic centers, $\psi_\Pi(\phi(p)^* \cap \phi(q)^*)$ is the image by ϕ of the set of all centers of these spheres. By definition of ψ_Π, it is the intersection of the hyperplane $\mathsf{H} = (\phi(p)^* \cap \phi(q)^*) \oplus \phi(\mathcal{H}_\infty)$ with Π.

The polar of this hyperplane is the point $\mathsf{H}^* = (\phi(p) \oplus \phi(q)) \cap \pi_\infty$, using Equation 1. Consequently, $\mathsf{H} \cap \Pi$ is the image by ϕ of a sphere in $\mathbb{E}^d$, which is the set of centers of spheres through p and q. All steps in the construction involve only rational computations. Figure 10 illustrates it for $d = 2$.

□

Since a k-face in $\mathrm{VD}_{\mathbb{H}}(\mathcal{P})$ is the bisector of k points of $\mathcal{P}$, it is the intersection of $k-1$ rational hyperplanes, we deduce that

Corollary 17 *The bisector of k points, for $2 \leq k \leq d$, is a hyperbolic $(d-k+1)$-flat whose equation is rational.*

For $k = d+1$, this means that the equation of a Voronoi vertex, seen as a Euclidean 0-sphere, is rational. However:

Proposition 18 *The coordinates of a hyperbolic Voronoi vertex are algebraic numbers of degree 2.*

Proof. There are at least two ways of seeing this result. One is to consider a hyperbolic Voronoi vertex as the intersection of d hyperplanes in $\mathbb{H}^d$, ie., d Euclidean spheres $S_0, \ldots, S_{d-1}$. This is

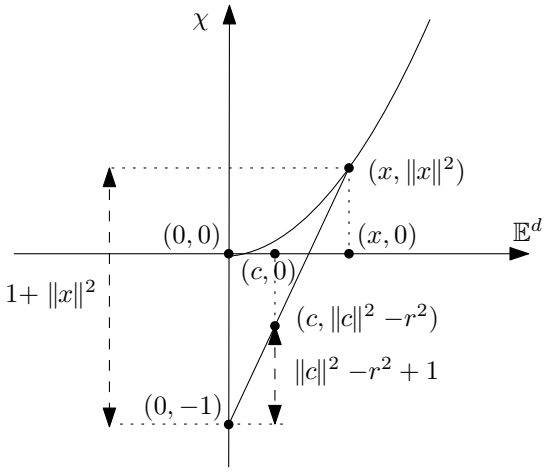

Figure 11: Computation of the hyperbolic center x of a sphere (c, r).

also the intersection of S_0 with the $d-1$ radical hyperplanes of S_0 and S_i, $1 \leq i < d$. Each radical hyperplane is rational, since its equation is obtained as the difference of the equations of the two corresponding spheres. The Voronoi vertex is the intersection point between a sphere and a line that lies in $\mathcal{B}$, which shows the result.

A direct construction of the hyperbolic center x of a sphere of Euclidean center c and radius r, using ψ_Π (see Figures 3 and 11), shows that $\|x\|$ is the smallest solution of $\|x\| = \frac{1+\|x\|^2}{1+c^2-r^2} \cdot \|c\|$, then,

$$x = \frac{1+\|x\|^2}{1+c^2-r^2} \cdot c.$$

□

The intersection of an infinite k-face of $\mathrm{VD}_{\mathbb{H}}(\mathcal{P})$ and $\mathcal{H}_\infty$ is a rational sphere. For $k = 1$, the intersection is a Euclidean 0-sphere on $\mathcal{H}_\infty$. Although, the equation of the 0-sphere is rational, the two points of the sphere have coordinates which are algebraic numbers of degree 2. To show this, it suffices to repeat the proof of Proposition 18 considering a point at infinity as the intersection of the sphere $\mathcal{H}_\infty$ and $d-1$ Euclidean spheres.

6 Implementation in $\mathbb{H}^2$

The construction of the Delaunay complex and the Voronoi diagram in $\mathbb{H}^2$ was implemented using CGAL [1]. The implementation will soon be submitted for future integration in CGAL. In this section, we first present the implementation, then we detail the computations used. We finally give some benchmarks.

6.1 Software design

CGAL library provides a package to compute the Delaunay triangulation and the Voronoi diagram in $\mathbb{E}^2$ [38]. First we give an introduction to the design of the package (a general presentation

of the CGAL design can be found in [23]). Then we discuss the design of our implementation for the hyperbolic case. We consider our implementation in terms of changes relative to the CGAL package.

6.1.1 CGAL 2D triangulations

The main class of the algorithm computing the Delaunay triangulation of $\mathbb{E}^2$ is `CGAL::Delaunay_triangulation_2<Gt, Tds>`. This class has two template parameters `Gt`, providing basic geometric computations, and `Tds`, handling combinatorical operations.

The geometric traits class `Gt` must provide a set of geometric objects, predicates and constructions that are required by the algorithm. Computing a Delaunay triangulation requires only predicates, namely `Orientation_2` and `In_circle_2` are the two main predicates. The computation of the Voronoi diagram requires geometric constructions such as `Construct_circumcenter_2`. The CGAL kernels provide all necessary predicates and constructions to compute Delaunay triangulation and Voronoi diagrams in $\mathbb{E}^2$ and can be used as traits class. The number type used for the computations can be chosen. A number type ensuring that predicates are evaluated exactly is required for the robust computation of the Delaunay triangulation. Constructions are only required for the Voronoi diagram and can be left approximate.

The second template parameter of the triangulation class is the triangulation data structure `Tds`, which maintains the combinatorial structure of the triangulation. It stores the vertices and the faces. A face stores three pointers to its vertices indexed from 0 to 2 and three pointers to its adjacent faces. A vertex stores a pointer to one of its incident faces. An edge is implicitly represented as a pair of an incident face and the index of the vertex that is opposite to the face. The class `CGAL::Triangulation_data_structure_2` provides a default implementation of `Tds`. It has two template parameters: a vertex class and a face class.

6.1.2 The 2D hyperbolic complex

Now we describe our implementation of the algorithm for computing the Delaunay complex in $\mathbb{H}^2$. We discuss the design as a whole. Then we turn to some specific aspects of the implementation.

Design

The class `Delaunay_hyperbolic_triangulation_2<Gt, Tds>` is derived from `CGAL::Delaunay_triangulation_2<Gt, Tds>`. It mainly consists of an implementation of extracting schemes of the hyperbolic complex from the Euclidean triangulation. Modifications in the classes used as template parameters are quickly mentioned below.

The geometric traits `Gt`. We introduce class `Triangulation_hyperbolic_traits_2<Kernel>` that provides the new predicate `is_hyperbolic`, as well as all geometric constructions (segments, circumcenters, bisectors, etc) in the hyperbolic plane. A CGAL kernel can be used as template parameter.

The triangulation data structure `Tds`. The same class `CGAL::Triangulation_data_structure_2` can be reused, enriching it with marks "hyperbolic" and "non-hyperbolic". Vertices of $\mathrm{DT}_{\mathbb{E}}(\mathcal{P})$ are always in $\mathrm{DT}_{\mathbb{H}}(\mathcal{P})$, so, they do not need to be marked. To be able to mark faces, we replace the default face class `CGAL::Triangulation_face_base_2` by a new class `Triangulation_hyperbolic_face_base_2`. The new class inherits from `CGAL::Triangulation_face_base_2` and maintains additional information. A Boolean is used to mark a face of $\mathrm{DT}_{\mathbb{E}}(\mathcal{P})$ as "hyperbolic" or "non-hyperbolic". To mark edges, we use the one-to-one correspondence between edges and faces of $\mathrm{DT}_{\mathbb{E}}(\mathcal{P})\backslash\mathrm{DT}_{\mathbb{H}}(\mathcal{P})$ defined in Corollary 7. Since each edge of a face is accessed through the index of the opposite vertex in the face, then it suffices to store also the index of the vertex opposite to the "non-hyperbolic" edge.

Extracting schemes
We implemented the two extracting schemes of the hyperbolic complex from the Euclidean triangulation described in Section 4.1.
Static scheme. The depth-first search of the graph G defined in Proposition 6 and marking its nodes are implemented as a private member function of the class `Delaunay_hyperbolic_triangulation_2<Gt, Tds>`. Since the static scheme first computes the whole Euclidean triangulation before performing the extraction, then the member function `insert(InputIterator first, InputIterator last)` of `Delaunay_hyperbolic_triangulation_2<Gt, Tds>` inherited from the base class `Delaunay_triangulation_2<Gt, Tds>` (denoted by `Base` below) is overridden as follows in the pseudo-code listing:

```
void insert(InputIterator first, InputIterator last) {
   Base::insert(InputIterator first, InputIterator last);
   mark_hyperbolic(); // depth-first search
}
```

Dynamic variant. At each insertion of a new point p, we first insert the point in the underlying Euclidean triangulation and then examine the star of p. The member function `insert(const Point& p, Face_handle start = Face_handle() )` is overridden as shown in the following pseudo-code (Σ is defined in Section 4.1 page 12):

```
Vertex_handle insert(const Point& p, Face_handle start = Face_handle() ) {
   Vertex_handle v = Base::insert(p, start);
   if each face of Σ is already marked ‘‘hyperbolic’’,
      then mark faces in star(v) as ‘‘hyperbolic’’
   else run is_hyperbolic on each face and edge of star(v);
   return v;
}
```

6.2 Algebraic and arithmetic aspects

Let us now detail the computations that are needed when implementing the algorithm.

6.2.1 Predicates

As already mentioned in Section 5.1, we rely on the CGAL package [38] to exactly compute the Euclidean Delaunay triangulation $\mathrm{DT}_{\mathbb{E}}(\mathcal{P})$. The hyperbolic complex $\mathrm{DT}_{\mathbb{H}}(\mathcal{P})$ is then extracted from $\mathrm{DT}_{\mathbb{E}}(\mathcal{P})$ using the predicate *is_hyperbolic* detailed in Sections 4.2 and 5.2. This predicate is called on Euclidean Delaunay triangles. Non-hyperbolic edges are deduced from non-hyperbolic triangles using the bijection introduced in Corollary 7.

Triangles
Let $pp'p''$ be a triangle of $\mathrm{DT}_{\mathbb{E}}(\mathcal{P})$ and $S_{pp'p''}$ its circumscribing circle. As noticed in Lemma 12, $\phi(S_{pp'p''}) = \phi(p)^* \cap \phi(p')^* \cap \phi(p'')^*$.

The equation of $\phi(p)^*$ is

$$\phi(p)^* : 2p_0x_0 + 2p_1x_1 - \chi = {p_0}^2 + {p_1}^2 \tag{4}$$

where (x_0, x_1, χ) is a point of $\mathbb{E}^3$.

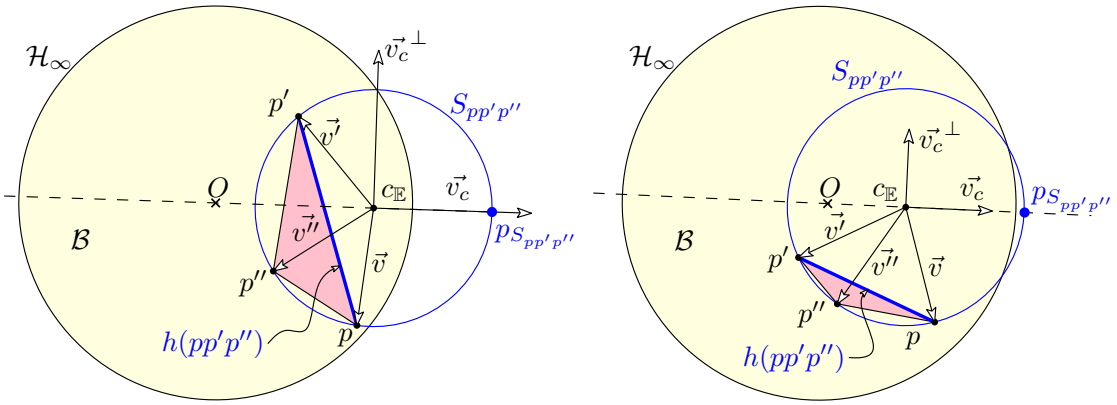

Figure 12: Determining the edge $h(pp'p'')$.

Solving the linear system $\phi(p)^*, \phi(p')^*, \phi(p'')^*$, we get

$$\phi(S_{pp'p''}) = \frac{1}{\begin{vmatrix} 2p_0 & 2p_1 & -1 \\ 2p'_0 & 2p'_1 & -1 \\ 2p''_0 & 2p''_1 & -1 \end{vmatrix}} \left(\begin{vmatrix} {p_0}^2+{p_1}^2 & 2p_1 & -1 \\ {p'_0}^2+{p'_1}^2 & 2p'_1 & -1 \\ {p''_0}^2+{p''_1}^2 & 2p''_1 & -1 \end{vmatrix}, \begin{vmatrix} 2p_0 & {p_0}^2+{p_1}^2 & -1 \\ 2p'_0 & {p'_0}^2+{p'_1}^2 & -1 \\ 2p''_0 & {p''_0}^2+{p''_1}^2 & -1 \end{vmatrix}, \begin{vmatrix} 2p_0 & 2p_1 & {p_0}^2+{p_1}^2 \\ 2p'_0 & 2p'_1 & {p'_0}^2+{p'_1}^2 \\ 2p''_0 & 2p''_1 & {p''_0}^2+{p''_1}^2 \end{vmatrix} \right) \tag{5}$$

Plugging this coordinates in Equation (3) describing the cone C we get that $S_{pp'p''}$ is hyperbolic if

$$\begin{vmatrix} {p_0}^2+{p_1}^2 & 2p_1 & -1 \\ {p'_0}^2+{p'_1}^2 & 2p'_1 & -1 \\ {p''_0}^2+{p''_1}^2 & 2p''_1 & -1 \end{vmatrix}^2 + \begin{vmatrix} 2p_0 & {p_0}^2+{p_1}^2 & -1 \\ 2p'_0 & {p'_0}^2+{p'_1}^2 & -1 \\ 2p'_0 & {p''_0}^2+{p''_1}^2 & -1 \end{vmatrix}^2 - \frac{1}{4}\left(\begin{vmatrix} 2p_0 & 2p_1 & -1 \\ 2p'_0 & 2p'_1 & -1 \\ 2p''_0 & 2p''_1 & -1 \end{vmatrix} + \begin{vmatrix} 2p_0 & 2p_1 & {p_0}^2+{p_1}^2 \\ 2p'_0 & 2p'_1 & {p'_0}^2+{p'_1}^2 \\ 2p''_0 & 2p''_1 & {p''_0}^2+{p''_1}^2 \end{vmatrix} \right)^2 < 0$$

that is

$$\begin{vmatrix} {p_0}^2+{p_1}^2 & p_1 & 1 \\ {p'_0}^2+{p'_1}^2 & p'_1 & 1 \\ {p''_0}^2+{p''_1}^2 & p''_1 & 1 \end{vmatrix}^2 + \begin{vmatrix} p_0 & {p_0}^2+{p_1}^2 & 1 \\ p'_0 & {p'_0}^2+{p'_1}^2 & 1 \\ p'_0 & {p''_0}^2+{p''_1}^2 & 1 \end{vmatrix}^2 - \begin{vmatrix} p_0 & p_1 & {p_0}^2+{p_1}^2-1 \\ p'_0 & p'_1 & {p'_0}^2+{p'_1}^2-1 \\ p''_0 & p''_1 & {p''_0}^2+{p''_1}^2-1 \end{vmatrix}^2 < 0$$

Thus we get the following lemma:

Lemma 19 *In $\mathbb{H}^2$, the predicate* is_hyperbolic *applied to a triangle can be evaluated as the sign of a polynomial of degree 8 in the coordinates of its vertices.*

Edges

Let $pp'p''$ be a triangle of $\mathrm{DT}_{\mathbb{E}}(\mathcal{P}) \setminus \mathrm{DT}_{\mathbb{H}}(\mathcal{P})$ with circumscribing circle $S_{pp'p''}$. The vertices p, p', p'' are given in counterclockwise order. Corollary 7 and Proposition 2 applied to $\mathrm{DT}_{\mathbb{E}}(\{p,p',p''\})$, yield that $h(pp'p'')$ is the unique edge in $\mathrm{DT}_{\mathbb{E}}(\{p,p',p''\}) \setminus \mathrm{DT}_{\mathbb{H}}(\{p,p',p''\})$.

Let $c_{\mathbb{E}}$ be the Euclidean center of $S_{pp'p''}$. We define the vectors $\vec{v} = p - c_{\mathbb{E}}$, $\vec{v'} = p' - c_{\mathbb{E}}$, $\vec{v''} = p'' - c_{\mathbb{E}}$, which verify $\|\vec{v}\|=\|\vec{v'}\|=\|\vec{v''}\|$ and $\vec{v}, \vec{v'}, \vec{v''}$ are in counterclockwise order.

Let us define $\vec{v_c} = \overrightarrow{Oc_{\mathbb{E}}}$. The vectors $\vec{v}, \vec{v'}, \vec{v''}$ split the circle $S_{pp'p''}$ into three (2D) spherical caps. The ray of origin $c_{\mathbb{E}}$ and direction $\vec{v_c}$ intersects $S_{pp'p''}$ in $p_{S_{pp'p''}}$, which lies in one of these three caps, and outside $\mathcal{B}$. The cap that contains $p_{S_{pp'p''}}$ is supported by $h(pp'p'')$ and can be

uniquely determined by the two vectors from $\vec{v}, \vec{v'}, \vec{v''}$ that define a wedge in counterclockwise order containing $\vec{v_c}$ (See Figure12).

The computation of $h(pp'p'')$ boils down to computing *Counterclockwise*$(\vec{v}, \vec{v_c}, \vec{v'})$, *Counterclockwise*$(\vec{v'}, \vec{v_c}, \vec{v''})$, and *Counterclockwise*$(\vec{v''}, \vec{v_c}, \vec{v})$, where *Counterclockwise*$(\vec{w}, \vec{v_c}, \vec{w'})$ tests whether the three vectors $\vec{w}, \vec{v_c}$, and $\vec{w'}$ are in counterclockwise order.[2]

It remains to detail the computation of *Counterclockwise*$(\vec{w}, \vec{v_c}, \vec{w'})$, where $\|w\|=\|w'\|$ (notice that $\|\vec{v_c}\|$ has no reason to be equal to $\|\vec{w}\|$). Let $\vec{v_c}^{\perp}$ be the vector obtained by rotating $\vec{v_c}$ by $\frac{\pi}{2}$. If $\text{sign}(\vec{w} \cdot \vec{v_c}^{\perp}) = -\text{sign}(\vec{w'} \cdot \vec{v_c}^{\perp}) = -1$ (which holds e.g. for $\vec{v}$ and $\vec{v'}$ in Figure 12-left) then *Counterclockwise*$(\vec{w}, \vec{v_c}, \vec{w'})$ is true. If $\text{sign}(\vec{w} \cdot \vec{v_c}^{\perp}) = \text{sign}(\vec{w'} \cdot \vec{v_c}^{\perp}) = -1$ (see Figure 12-right) then *Counterclockwise*$(\vec{w}, \vec{v_c}, \vec{w'})$ is equal to *Orientation*$(\vec{w}, \vec{v_c}, \vec{w'})$. Other cases are symmetric.

From Equation (5)

$$c_{\mathbb{E}} = \frac{1}{\begin{vmatrix} 2p_0 & 2p_1 & -1 \\ 2p'_0 & 2p'_1 & -1 \\ 2p''_0 & 2p''_1 & -1 \end{vmatrix}} \left(\begin{vmatrix} {p_0}^2+{p_1}^2 & 2p_1 & -1 \\ {p'_0}^2+{p'_1}^2 & 2p'_1 & -1 \\ {p''_0}^2+{p''_1}^2 & 2p''_1 & -1 \end{vmatrix}, \begin{vmatrix} 2p_0 & {p_0}^2+{p_1}^2 & -1 \\ 2p'_0 & {p'_0}^2+{p'_1}^2 & -1 \\ 2p'_0 & {p''_0}^2+{p''_1}^2 & -1 \end{vmatrix} \right).$$

So, the coordinates of $\vec{v}$, $\vec{v'}$, $\vec{v''}$, and $\vec{v_c}$ are rational fractions with numerators of degree 3 and a common denominator of degree 2. Thus the signs of the above scalar products and *Orientation* tests boil down to signs of polynomials of degree 6, and we get the following lemma:

Lemma 20 *The non hyperbolic edge associated to a non hyperbolic triangle by the map h can be determined by the evaluation of the signs of polynomials of degree 6 in the coordinates of its vertices.*

Exact evaluation

We have seen that all predicate evaluations boil down to computing signs of polynomials. As for the CGAL Euclidean Delaunay triangulations (section 5.1), this can be done in a fast and exact way using filtered exact computations, providing an efficient and fully robust implementation.

6.2.2 Constructions

To draw the Delaunay triangulation we need to construct the hyperbolic line through two points, and for and the Voronoi diagram we need to construct the hyperbolic bisector of two points and the hyperbolic center of the circle through three points.

Hyperbolic line

The hyperbolic line through p and p' is supported by the Euclidean circle S through p, p', and orthogonal to $\mathcal{B}$:

$$\begin{aligned}
\phi(S) &= \phi(p)^* \cap \phi(p')^* \cap \pi_\infty \\
&= \frac{1}{\begin{vmatrix} p_0 & p_1 & -1 \\ p'_0 & p'_1 & -1 \\ 0 & 0 & 1 \end{vmatrix}} \left(\begin{vmatrix} {p_0}^2+{p_1}^2 & p_1 & -1 \\ {p'_0}^2+{p'_1}^2 & p'_1 & -1 \\ 1 & 0 & 1 \end{vmatrix}, \begin{vmatrix} p_0 & {p_0}^2+{p_1}^2 & -1 \\ p'_0 & {p'_0}^2+{p'_1}^2 & -1 \\ 0 & 1 & 1 \end{vmatrix}, \begin{vmatrix} p_0 & p_1 & {p_0}^2+{p_1}^2 \\ p'_0 & p'_1 & {p'_0}^2+{p'_1}^2 \\ 0 & 0 & 1 \end{vmatrix} \right) \\
&= \left(-\frac{\begin{vmatrix} p_1 & {p_0}^2+{p_1}^2-1 \\ p'_1 & {p'_0}^2+{p'_1}^2-1 \end{vmatrix}}{p'_0p_1 - p_0p'_1}, \frac{\begin{vmatrix} p_0 & {p_0}^2+{p_1}^2-1 \\ p'_0 & {p'_0}^2+{p'_1}^2-1 \end{vmatrix}}{p'_0p_1 - p_0p'_1}, 1 \right).
\end{aligned}$$

[2] Degeneracies in the *Counterclockwise* test cannot occur since they would correspond either to equality of two points of $\{p, p', p''\} \subset \mathcal{B}$ or equality of one of these points to $p_{S_{pp'p''}} \notin \mathcal{B}$.

Hyperbolic bisector
As noticed in the proof of Lemma 16, the hyperbolic bisector of p and p' is suported by the Euclidean circle S such that $\phi(S) = line(\phi(p), \phi(p')) \cap \pi_\infty$.

$$\phi(S) = \frac{{p'_0}^2 + {p'_1}^2}{2({p_0}^2 + {p_1}^2)({p'_0}^2 + {p'_1}^2)}(p_0, p_1, {p_0}^2 + {p_1}^2) + \frac{{p_0}^2 + {p_1}^2}{2({p_0}^2 + {p_1}^2)({p'_0}^2 + {p'_1}^2)}(p'_0, p'_1, {p'_0}^2 + {p'_1}^2)$$

Hyperbolic circumcenter
As observed in the proof of Proposition 18 the hyperbolic center x of the triangle $pp'p''$ can be computed as $\psi_\Pi(\phi(p)^* \cap \phi(p')^* \cap \phi(p'')^*)$.

Let $\frac{1}{\delta}(\alpha, \beta, \gamma)$ be $\phi(p)^* \cap \phi(p')^* \cap \phi(p'')^*)$, we have already computed in Equation 5

$$\delta = \begin{vmatrix} 2p_0 & 2p_1 & -1 \\ 2p'_0 & 2p'_1 & -1 \\ 2p''_0 & 2p''_1 & -1 \end{vmatrix}, \quad \alpha = \begin{vmatrix} {p_0}^2 + {p_1}^2 & 2p_1 & -1 \\ {p'_0}^2 + {p'_1}^2 & 2p'_1 & -1 \\ {p''_0}^2 + {p''_1}^2 & 2p''_1 & -1 \end{vmatrix},$$

$$\beta = \begin{vmatrix} 2p_0 & {p_0}^2 + {p_1}^2 & -1 \\ 2p'_0 & {p'_0}^2 + {p'_1}^2 & -1 \\ 2p'_0 & {p''_0}^2 + {p''_1}^2 & -1 \end{vmatrix}, \quad \gamma = \begin{vmatrix} 2p_0 & 2p_1 & {p_0}^2 + {p_1}^2 \\ 2p'_0 & 2p'_1 & {p'_0}^2 + {p'_1}^2 \\ 2p''_0 & 2p''_1 & {p''_0}^2 + {p''_1}^2 \end{vmatrix}$$

then let λ be the smallest solution of $\lambda^2 + \frac{\gamma - \delta}{\sqrt{\alpha^2 + \beta^2}}\lambda - 1 = 0$ that is

$$\lambda = -\frac{\gamma - \delta}{\sqrt{4\alpha^2 + 4\beta^2}} - \sqrt{\frac{\delta^2 - 2\delta\gamma + \gamma^2}{4\alpha^2 + 4\beta^2} - 1} = \frac{\delta - \gamma - \sqrt{(\gamma - \delta)^2 - 4\alpha^2 - 4\beta^2}}{\sqrt{4\alpha^2 + 4\beta^2}}$$

and the hyperbolic center is

$$x = \frac{1 + \lambda^2}{\delta(1 + \gamma)}(\alpha, \beta).$$

Evaluation
CGAL provides us with number type `Sqrt_extension` for exact computations on algebraic numbers of degree 2 [24], allowing us to construct in an exact way the hyperbolic center of a circle as well as hyperbolic bisector between two input points. These constructions are rounded only when displaying the hyperbolic Voronoi diagram.

6.3 Experimental results

Experiments are run on point sets $\mathcal{P}$ that are uniformly distributed (up to rounding errors when generating them) *according to the hyperbolic metric* in open balls in $\mathcal{B}$ (See Figure 13). Each open ball is centered at the origin of $\mathcal{B}$ with Euclidean radius $1 - \epsilon$. The point sets in the open balls are denoted by `small_sph` for $\epsilon = 0.001$ and by `big_sph` for $\epsilon = 0.0000001$.

We insert all points in $\mathcal{P}$ at once, and we measure the running times of the computations of $\mathrm{DT}_{\mathbb{E}}(\mathcal{P})$ with the CGAL implementation [38] and of $\mathrm{DT}_{\mathbb{H}}(\mathcal{P})$ with our implementation. This allows us to measure the overhead due the static extraction of the Delaunay complex in $\mathbb{H}^2$.

The tables for the results are organized as follows. The first column gives the number of input points. The second and the third column give running times in seconds for the computations

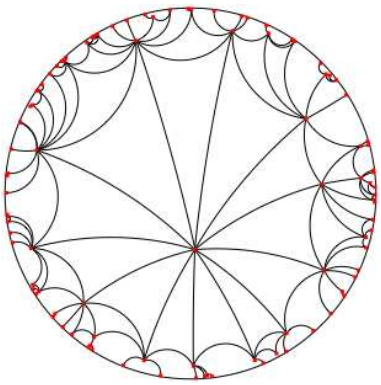

Figure 13: 100 uniformly distributed points in an open ball in $\mathbb{H}^2$.

of $\mathrm{DT}_{\mathbb{E}}(\mathcal{P})$ and $\mathrm{DT}_{\mathbb{H}}(\mathcal{P})$, respectively. The fourth column shows the overhead factor of the computation of $\mathrm{DT}_{\mathbb{H}}(\mathcal{P})$ compared to $\mathrm{DT}_{\mathbb{E}}(\mathcal{P})$.

Experiments are conducted on a MacBookPro 2.6 GHz running CGAL 4.0 in release mode, using GCC 4.2. Running times are averaged on 10 trials. For both $\mathrm{DT}_{\mathbb{E}}(\mathcal{P})$ and $\mathrm{DT}_{\mathbb{H}}(\mathcal{P})$, we use `CGAL::Exact_predicates_inexact_constructions_kernel`, which provides filtered exact geometric predicates.

We run experiments by inserting all points in $\mathcal{P}$ at once, and we measure the overhead of the static extraction of the Delaunay complex in $\mathbb{H}^2$ compared to the computation of the 2D Delaunay triangulation in $\mathbb{E}^2$ by the CGAL implementation.

`small_sph`	$\mathbb{E}^2$	$\mathbb{H}^2$	factor
10^4	0.0078133	0.011175	1.43
10^5	0.0836044	0.101224	1.21
10^6	0.893011	0.987953	1.1
10^7	9.55691	10.3007	1.07

`big_sph`	$\mathbb{E}^2$	$\mathbb{H}^2$	factor
10^4	0.0074206	0.0184465	2.48
10^5	0.0824148	0.181072	2.19
10^6	0.899058	1.14592	1.27
10^7	9.75887	11.1625	1.14

We observe that the overhead of the extraction decreases with the size of the input point set. The reason is that the graph of faces that is traversed by the extraction scheme grows slower than the whole graph of the Euclidean triangulation. Faces examined during the extraction are in some sense "close" to the convex hull of the point set.

As could be expected, for `small_sph`, even for small point sets, the overhead is already similar to the overhead obtained on `big_sph` for large point sets, since a small fraction of Euclidean Delaunay circles intersect $\mathcal{H}_\infty$.

We also observed that the ratio *(# edges in $DT_{\mathbb{E}}(\mathcal{P})$) / (# edges in $DT_{\mathbb{H}}(\mathcal{P})$)* quickly decreases with the number of vertices. For instance, on `big_sph` with 10^7 points, this ratio is 1.006.

7 Conclusion and Open Problems

We proposed a algorithm to compute hyperbolic Voronoi diagrams and Delaunay complexes, as well as a complete and efficient implementation, to be submitted to CGAL.

We are pursuing research on periodic hyperbolic Delaunay triangulations, in the flavor of what we had proposed for the Euclidean case [11, 12]. This is motivated by applications in various fields such as geometry processing [31] and neuro mathematics [22].

References

[1] CGAL, Computational Geometry Algorithms Library. http://www.cgal.org.

[2] F. Aurenhammer. Voronoi diagrams: A survey of a fundamental geometric data structure. *ACM Comput. Surv.*, 23(3):345–405, September 1991.

[3] Franz Aurenhammer and Rolf Klein. Voronoi diagrams. In Jörg-Rüdiger Sack and Jorge Urrutia, editors, *Handbook of Computational Geometry*, pages 201–290. Elsevier Science Publishers B.V. North-Holland, Amsterdam, 2000. http://wwwpi6.fernuni-hagen.de/Publikationen/tr198.pdf.

[4] A. F. Beardon. *The Geometry of Discrete Groups*. Graduate Texts in Mathematics. Springer-Verlag, 1983.

[5] M. Berger. *Geometry (vols. 1-2)*. Springer-Verlag, 1987.

[6] M. Bern and D. Eppstein. Optimal Möbius transformations for information visualization and meshing. In *7th Worksh. Algorithms and Data Structures*, volume 2125 of *Lecture Notes in Comp. Sci.*, Providence, Rhode Island, USA, 2001. Springer-Verlag. http://arxiv.org/abs/cs.CG/0101006.

[7] Mikhail Bogdanov, Olivier Devillers, and Monique Teillaud. Hyperbolic Delaunay triangulations and Voronoi diagrams made practical. In *Abstracts XIV Spanish Meeting on Computational Geometry*, pages 113–116, 2011. http://www2.uah.es/egc2011/files/ActasEGC2011.pdf.

[8] Jean-Daniel Boissonnat, André Cérézo, Olivier Devillers, and Monique Teillaud. Output-sensitive construction of the Delaunay triangulation of points lying in two planes. *Internat. J. Comput. Geom. Appl.*, 6(1):1–14, 1996. http://www-sop.inria.fr/prisme/publis/bcdt-oscdt-96.ps.gz.

[9] Jean-Daniel Boissonnat and Mariette Yvinec. *Algorithmic Geometry*. Cambridge University Press, UK, 1998. Translated by Hervé Brönnimann. http://www.cup.cam.ac.uk/Scripts/webbook.asp?isbn=0521563224.

[10] A. Bowyer. Computing Dirichlet tesselations. *Comput. J.*, 24:162–166, 1981. http://comjnl.oxfordjournals.org/content/24/2/162.short.

[11] Manuel Caroli and Monique Teillaud. Computing 3d periodic triangulations. In *European Symposium on Algorithms*, volume 5757 of *Lecture Notes in Computer Science*, pages 37–48, 2009. http://www.springerlink.com/content/55415144316j214g/fulltext.pdf.

[12] Manuel Caroli and Monique Teillaud. Delaunay triangulations of point sets in closed Euclidean d-manifolds. In *Proc. 27th Annual Symposium on Computational Geometry*, pages 274–282, 2011. http://doi.acm.org/10.1145/1998196.1998236.

[13] Mark de Berg, Marc van Kreveld, Mark Overmars, and Otfried Schwarzkopf. *Computational Geometry: Algorithms and Applications*. Springer-Verlag, Berlin, 1997. http://www.cs.ruu.nl/geobook/.

[14] Olivier Devillers. The Delaunay hierarchy. *Internat. J. Found. Comput. Sci.*, 13:163–180, 2002. http://hal.inria.fr/inria-00166711.

[15] Olivier Devillers, Stefan Meiser, and Monique Teillaud. The space of spheres, a geometric tool to unify duality results on Voronoi diagrams. In *Proc. 4th Canad. Conf. Comput. Geom.*, pages 263–268, 1992. Long version: Report 1620, INRIA, 1992. http://hal.inria.fr/inria-00074941.

[16] Olivier Devillers and Sylvain Pion. Efficient exact geometric predicates for Delaunay triangulations. In *Proc. 5th Workshop Algorithm Eng. Exper.*, pages 37–44, 2003.

[17] Olivier Devillers, Sylvain Pion, and Monique Teillaud. Walking in a triangulation. *Internat. J. Found. Comput. Sci.*, 13:181–199, 2002. http://hal.inria.fr/inria-00102194/.

[18] Olivier Devillers and Monique Teillaud. Perturbations for Delaunay and weighted Delaunay 3D triangulations. *Computational Geometry: Theory and Applications*, 44:160–168, 2011. http://hal.archives-ouvertes.fr/inria-00560388/.

[19] H. Edelsbrunner and R. Seidel. Voronoi diagrams and arrangements. *Discrete Comput. Geom.*, 1:25–44, 1986.

[20] D. Eppstein. Hyperbolic geometry, Möbius transformations, and geometric optimization, 2003. Invited talk at MSRI Introductory Workshop on Discrete and Computational Geometry.

[21] D. Eppstein and M. T. Goodrich. Succinct greedy graph drawing in the hyperbolic plane. In *Proc. 16th Int. Symp. Graph Drawing*, volume 5417 of *Lecture Notes in Computer Science*, pages 14–25, Heraklion, Crete, 2008. IEEE Transactions on Computing. http://arxiv.org/abs/0806.0341.

[22] G. Faye, P. Chossat, and O. Faugeras. Some theoretical results for a class of neural mass equations. Technical report, 2010. http://arxiv.org/abs/1005.0510.

[23] Efi Fogel and Monique Teillaud. Generic programming and the CGAL library. In Jean-Daniel Boissonnat and Monique Teillaud, editors, *Effective Computational Geometry for Curves and Surfaces*. Springer-Verlag, Mathematics and Visualization, 2006.

[24] Michael Hemmer, Susan Hert, Lutz Kettner, Sylvain Pion, and Stefan Schirra. Number types. In *CGAL User and Reference Manual*. CGAL Editorial Board, 4.1 edition, 2012. http://www.cgal.org/Manual/4.1/doc_html/cgal_manual/packages.html#Pkg:NumberTypes.

[25] M.K. Hurdal and K. Stephenson. Cortical cartography using the discrete conformal approach of circle packings. *Neuroimage*, 23:119–128, 2004.

[26] M. Jin, J. Kim, F. Luo, and X. Gu. Discrete surface Ricci flow. *IEEE Trans. Vis. Comput. Graph.*, 14(5):1030–1043, 2008.

[27] Tamara Munzner. Exploring large graphs in 3D hyperbolic space. *IEEE Computer Graphics and Applications*, 18(4):18–23, 1998.

[28] Frank Nielsen and Richard Nock. Hyperbolic Voronoi diagrams made easy. In *Proc. 10th International Conference on Computational Science and its Applications*, pages 74–80, Los Alamitos, CA, USA, 2010. IEEE Computer Society. http://doi.ieeecomputersociety.org/10.1109/ICCSA.2010.37.

[29] K. Onishi and N. Takayama. Construction of Voronoi diagrams on the upper half-plane. *IEICE Trans. Fundamentals*, E79-A(4):533–539, 1996.

[30] Sylvain Pion and Monique Teillaud. 3D triangulations. In *CGAL User and Reference Manual*. CGAL Editorial Board, 4.1 edition, 2012. http://www.cgal.org/Manual/4.0/doc_html/cgal_manual/packages.html#Pkg:Triangulation3.

[31] Guodong Ron, Miao Jin, and Xiaohu Guo. Hyperbolic centroidal Voronoi tessellation. In *Proc. ACM Symposium on Solid and Physical Modeling*, pages 117–126, Haifa, Israel, 2010.

[32] Toshihiro Tanuma, Hiroshi Imai, and Sonoko Moriyama. Revisiting hyperbolic Voronoi diagrams from theoretical, applied and generalized viewpoints. *International Symposium on Voronoi Diagrams in Science and Engineering*, pages 23–32, 2010.

[33] W. P. Thurston. Three dimensional manifolds, Kleinian groups, and hyperbolic geometry. *Bull. Amer. Math. Soc.*, 6(3):357–381, 1982.

[34] William P. Thurston. *The Geometry and Topology of Three-Manifolds*. 2002. http://www.msri.org/publications/books/gt3m/.

[35] D. F. Watson. Computing the n-dimensional Delaunay tesselation with applications to Voronoi polytopes. *Comput. J.*, 24(2):167–172, 1981. http://comjnl.oxfordjournals.org/content/24/2/167.short.

[36] P M. H. Wilson. *Curved Spaces*. Cambridge University Press, Cambridge, 2008.

[37] C. K. Yap and T. Dubé. The exact computation paradigm. In D.-Z. Du and F. K. Hwang, editors, *Computing in Euclidean Geometry*, volume 4 of *Lecture Notes Series on Computing*, pages 452–492. World Scientific, Singapore, 2nd edition, 1995. http://cs.nyu.edu/cs/faculty/yap/papers/paradigm.ps.

[38] Mariette Yvinec. 2D triangulations. In *CGAL User and Reference Manual*. CGAL Editorial Board, 4.1 edition, 2012. http://www.cgal.org/Manual/4.0/doc_html/cgal_manual/packages.html#Pkg:Triangulation2.

[39] W. Zeng, R. Sarkar, F. Luo, X. Gu, and J. Gao. Resilient routing for sensor networks using hyperbolic embedding of universal covering space. In *Proceedings of the 29th conference on Information communications*, INFOCOM'10, pages 1694–1702, Piscataway, NJ, USA, 2010. IEEE Press.

RESEARCH CENTRE
SOPHIA ANTIPOLIS – MÉDITERRANÉE

2004 route des Lucioles - BP 93
06902 Sophia Antipolis Cedex

Publisher
Inria
Domaine de Voluceau - Rocquencourt
BP 105 - 78153 Le Chesnay Cedex
inria.fr

ISSN 0249-6399